DOI: 10.24996/ijs.2026.67.2.9

ISSN: 0067-2904

Biological Activity of the Selenium Nanoparticles Prepared by *Saccharomyces cerevisiae* Extract Against Methicillin-Resistant *Staphylococcus aureus*

Maarib Mudhar Farouq, Zina Hashem Shehab*

Department of Biology, College of Science for Women, University of Baghdad , Iraq

Received:10/9/2024 Accepted:4/2/2025 Published: 28/2/2026

Abstract

There is increased interest in using safe substances for human health, such as creating nanoparticles in an easy and affordable manner to solve the issue of antibiotic resistance. The purpose of this study was to create a new antibacterial agent by using *Saccharomyces cerevisiae* extract (ScE) to biosynthesize selenium nanoparticles (SeNPs), that inhibit the growth of methicillin-resistant *Staphylococcus aureus* (MRSA). From 150 swabs taken from various clinical sources from patients at several hospitals in Baghdad, thirty-six *S. aureus* were isolated and diagnosed based on phenotypic characteristics, biochemical tests and then confirmed by PCR via targeting *16S rRNA* gene for *S. aureus*, and *mecA* for methicillin-resistant *S. aureus* diagnosis. Following the use of several appropriate techniques, including FTIR, UV–vis, AFM, fe-SEM, and XRD, selenium nanoparticles (Sc-SeNPs) were shown to be a chemically stable materials with highly crystalline spherical particles and a maximum grain size of 54.04 nm. A GC-MS analysis was carried out to determine the important active chemicals in the *S. cerevisiae* extract. Sc-SeNPs appear to offer new viewpoints on their biological efficacy as agents that inhibit bacterial growth and biofilms. This result shows that it has medicinal importance. Therefore, biogenic SeNPs seem to be promising candidates for safe medical use, either by themselves or in combination with conventional biogenic compounds, to inhibit the growth of clinical isolates of *S. aureus* or to make it easier for antimicrobial drugs to penetrate *S. aureus* biofilms.

Keywords: Antibacterial, Antibiofilm, MRSA, Selenium nanoparticles, *Saccharomyces cerevisiae*.

النشاط البيولوجي لدقائق السيلينيوم النانوية المحضرة بواسطة مستخلص الخميرة ضد المكورات العنقودية الذهبية المقاومة للميثيسيلين

مآرب مضر فاروق ,زينه هاشم شهاب*

قسم علوم الحياة , كلية العلوم للبنات , جامعة بغداد , العراق

الخلاصة

هناك اهتمام متزايد باستخدام المواد الآمنة على صحة الإنسان لتخليق دقائق نانوية بطريقة سهلة وبأسعار معقولة لحل مشكلة مقاومة المضادات الحيوية. ان الغرض من هذه الدراسة انتاج عوامل جديدة مضادة للبكتيريا

*Email: zinahs_bio@csw.uobaghdad.edu.iq

باستخدام مستخلصScE) *Saccharomyces cerevisiae*) لتخليق دقائق السيلينيوم النانوية (SeNPs)، والتي تمنع نمو المكورات العنقودية الذهبية المقاومة للميثيسيلين (MRSA). من 150 عينة مأخوذة من مصادر سريرية مختلفة لمرضى لعدد من مستشفيات بغداد، تم عزل ستة وثلاثون عزلة من المكورات العنقودية الذهبية وتشخيصها بناءً على الخصائص المظهرية والاختبارات الكيميائية الحيوية ثم تم تأكيدها من خلال تفاعل البوليميراز المتسلسل ((PCRلجين *16S rRNA* لتشخيص المكورات العنقودية الذهبية، و*mecA* لتشخيص المكورات العنقودية الذهبية المقاومة للميثيسيلين. وبعد استخدام العديد من التقنيات المناسبة، بما في ذلك FTIR وUV–vis وAFM و fe–SEMوXRD، تبين أن دقائق السيلينيوم النانوية (Sc–SeNPs) هي مواد مستقرة كيميائيًا مع جزيئات كروية شديدة التبلور وحجم حبيبات أقصى يبلغ 54.04 نانومتر. ولتحديد المواد الكيميائية النشطة المهمة في مستخلص*S. cerevisiae* ، تم إجراء تحليل كروموتوغرافيا الغاز . ويبدو أن دقائق السيلينيوم النانوية تقدم وجهات نظر جديدة بشأن فعاليتها البيولوجية كعوامل تثبط نمو البكتيريا والأغشية الحيوية . وتشير هذه النتجة إلى أنها ذات أهمية طبية وبالتالي، يبدو أن دقائق السيلينيوم النانوية الحيوية مرشحة واعدة للاستخدام الطبي الآمن، سواء بمفردها أو بالاشتراك مع بعض المركبات الحيوية ، لتثبيط نمو العزلات السريرية من المكورات العنقودية الذهبية أو لتسهيل اختراق الأدوية المضادة للميكروبات للأغشية الحيوية للمكورات العنقودية الذهبية.

1- Introduction

Staphylococcus aureus is a persistent pathogen in humans and animals and is responsible for a wide range of infections that differ broadly in clinical manifestations and severity. Moreover, *S. aureus* elaborates on a collection of cell wall-associated proteins that have the ability to interact with host extracellular matrix proteins. Therefore, it is assumed to play a crucial role in both colonization and invasion [1]. Biofilms are collections of single-celled bacteria that stick to inert surfaces to build multicellular formations. Pathogenic bacteria can grow as biofilms on the inert surfaces of implanted devices, including joint replacements, prosthetic heart valves, and catheters [2]. The formation of biofilms in vivo by *S. aureus* is thought to be a primary virulence factor that impacts its pathogenicity. Diabetes-related dietary and prosthetic hip infections have been linked to high rates of biofilm formation and increased resistance to antibiotics [3]. Furthermore, a variety of illnesses in both human and animal hosts are caused by staphylococcal infections, which are related to programmed cell death [4]. A single-celled fungus called *Saccharomyces cerevisiae* is also referred to as baker's yeast [5]. For most fundamental research initiatives in eukaryotic organisms, *S. cerevisiae*, the most studied eukaryote, is a valuable resource. This is because *S. cerevisiae* is a unicellular organism, which often makes things easier to understand and combines nearly every biological function seen in eukaryotes with those that are highly conserved in *S. cerevisiae*. Additionally, genetic modification works well with it. *S. cerevisiae* is also crucial for a variety of biotechnological applications, some of which date back thousands of years, in contrast to other model organisms. *S. cerevisiae* has certain biological characteristics that make it useful for biotechnological applications, such as its capacity to ferment and create CO_2 and alcohol [6]. Currently, metabolomic analysis is conducted via various analytical technologies, such as gas chromatography coupled with mass spectrometry (GC–MS)[7].

Nanotechnology facilitates access to further sensitive and successful ways of treating bacterial illnesses as a result of the rise in antimicrobial resistance. Researchers can create nanoparticles smaller than 100 nanometers in at least one dimension and employ them for a range of purposes owing to nanotechnology. Furthermore, in comparison with traditional micron-sized particles, nanoparticles have larger surface areas and, as a result, interact with biological targets such as bacteria more frequently. Moreover, compared with microparticles,

nanoparticles enter cells more readily [8]. Numerous medical applications, including anticancer applications, have been researched for selenium. It has been demonstrated that taking supplements containing selenium can lower the chance of developing certain malignancies [9]. Organoselenium compound sequences have been created and demonstrated to exhibit antibacterial properties in vitro, with a specific focus on *Staphylococcus aureus* [10]. The study aimed to determine the bioactivity of an *S. cerevisiae* extract loaded with selenium nanoparticles as an antibacterial and antibiofilm agent for the *S. aureus* bacterium.

2-Materials and methods

2-1 Sample collection and identification

Between November 2023 and March 2024, one hundred fifty samples from several clinical sources (wound, urine, burn, sputum, nasal swabs, throat swabs and CSF), were collected from patients between the ages of 13 and 80 years from both genders visiting Baghdad hospitals (Al-Kindy teaching hospitals, Imam al-Kazem in city teaching hospitals, Ghazi Al-Harery hospitals, specialized burning hospitals, and Al-Karkh general hospitals). All the samples were directly inoculated into blood agar and incubated overnight at 37°C. Using Gram staining, catalase tests, coagulase tests, and growth on mannitol salt agar (MSA) as a selective medium, colonies on culture plates were identified and verified as *S. aureus*, according to Bergey's manual [11]. We subsequently confirmed the identification of thirty-six isolates that were positive for cultural and biochemical tests and genotypic detection via the PCR technique. *16S rRNA* was used for *S. aureus* diagnosis, and *mecA* was used for methicillin-resistant *S. aureus* diagnosis in the Department of Biology, College of Science for Women, University of Baghdad's laboratories.

2-2 Molecular identification by PCR assay

Genomic DNA was extracted from 36 bacterial isolates using the HiPurA® bacterial genomic DNA purification kit following the manufacturer's instructions. The *16S rRNA* gene was amplified using primers *16S rRNA* -F-`5'- AACCTACCTATAAGACTGGG'-3` and *16S rRNA* -R-`5'- CATTTCACCGCTACACATGG -3`. While the *mecA* gene was amplified using primers *mecA* -F-5'- ACTGCTATCCACCCTCAAAC -3' and *mecA*-R-5'- CTGGTGAAGTTGTAATCTGG -3', which produced a 578 and 163 bps amplicon respectively [12,13]. The (25µl) PCR volume consists of (6.5µl) nuclease-free water, (1µl) each of forward and reverse primers, (1µl) of extracted template DNA and (12.5µl) of master mix (2X). The amplification was performed in a PCR thermal cycler of initial denaturation at 94°C for 5 minutes followed by 35 cycles of amplification (denaturation at 94°C for 20 seconds, annealing at 55°C for 45 seconds, and elongation at 72°C for 45 seconds), ending with a final extension at 72°C for 10 minutes. The PCR products were run on 1.5% agarose gel (70 volts for 80 min.) with ethidium bromide dye and, visualized under an ultraviolet transilluminator and photographed. This is for the *16SrRNA* gene, while for the *mecA* gene, it was initial denaturation at 94°C for 5 minutes followed by 35 cycles of amplification (denaturation at 94°C for 2 min, annealing at 57°C for 2 min, and elongation at 72°C for 1 min), ending with a final extension at 72°C for 7 min. The PCR products were run on 1.5% agarose gel (70 volts for 75 min.) with ethidium bromide dye and, visualized under an ultraviolet transilluminator, and photographed [12,13]

2-3 Preparation and identification of S. cerevisiae

Yeast *S. cerevisiae* was taken from commercial dried Baker Yeast (produced in Turkey by Lesaffre turquie Mayacilik) and purchased from the local markets in Baghdad/ Iraq. One ml of

the sample was transferred to 9 ml of sterile normal saline water and mixed thoroughly. It was inoculated on to potato dextrose agar (PDA) plates. The sample was incubated at 30 ºC for 48 hrs. The yeast strain was identified on the basis of its cultural traits (colony shape, color, and smell). The yeast was characterized depending on morphological features on culture media and microscopic examination. According to Barnett. [14]. The identification was then verified by genotypic detection employing conventional PCR and sequencing technology

2-4 Molecular identification of S. cerevisiae via PCR.

Following the manufacturer's instructions, genomic DNA was isolated from the S. cerevisiae isolate via an ABIO PureTM fungal genomic DNA purification kit. The primers *ITS1* (5`-TCCGTAGGTGAACCTGCGG-3`) and *ITS4* (5`-TCCTCCGCTTATTGATATGC-3`) were used to amplify the *ITS* gene with an amplicon of 880 bps. The (25 µl) PCR mixture consisted of 12.5 µl of master mix (2X), 2 µl of extracted template DNA, 1 µl of forward and reverse primers, and 8.5 µl of nuclease-free water. In a PCR thermal cycler, the amplification was performed by first denaturing at 95°C for five minutes, followed by 30 cycles of amplification (denaturing for 30 seconds at 95°C, annealing for 30 seconds at 55°C, and elongating for 30 seconds at 72°C). Following a final extension at 72°C for 7 min, the PCR products were run on a 1.5% agarose gel at 100 v/mAmp for 60 min. The gel imaging equipment was used to visualize the gel's ethidium bromide-stained bands [15].

2-5 Preparation of S. cerevisiae medium

The baker's yeast (*S. cerevisiae*) was cultured in a medium (g L-1), as described previously by Ruiz-Marín *et al.,* [16], with some modifications: 1.8 g of glucose, 0.92 g of $CaCl_2.2H_2O$, 16 g of $(NH_4)2SO_4$, 4 g of $MgSO_4.7H_2O$, and 6 g of autoclaved KH_2PO_4. The yeasts were maintained in 3 L of culture media (1 g of yeast per liter) at 30°C and pH 4.5 with shaking in an incubator shaker for two days. The selected culture medium allows the favored growth of yeast.

2-6 Preparation of S. cerevisiae extract (ScE)

Yeast free-cell extracts were prepared according to the method of Zareia, *et al.,* [17]. The previously prepared growth suspension was separated via centrifugation at 4000 rpm for 10min. The cell-free supernatant was incubated at 4°C for 10 min, after it was collected. The supernatant was recentrifuged again under the same conditions to ensure that the insoluble cell contents were removed. The cell-free yeast supernatant was extracted by placing 500 ml of it in a rotary evaporator at 80°C until the excess water was removed and the remaining was placed in a glass Petri dish in an oven at 40°C to dry.

2-7 Gas-chromatography–mass spectrometry (GC–MS) analysis

At the Ministry of Science and Technology, a gas chromatography mass spectrometer (Shimadzu QP-2010 plus) from Japan, was used to identify the active compounds in the *S. cerevisiae* extract. This was accomplished by comparing the absorbance's of the unknown compounds with those stored and known components in the National Institute of Standards and Technology (NIST) library.

2-8 Biosynthesis of selenium nanoparticles aqueous S. cerevisiae extract (Sc-SeNPs)

S. cerevisiae extracts loaded on selenium nanoparticles were synthesized in accordance with the methods of Salem *et al*., [18]. Ninety milliliters of 2 mM $NaHSeO_3$ and 10 ml of aqueous *S. cerevisiae* extract were dripped separately, drop wise, at a flow rate of 0.2 ml/min. This reaction

mixture allowed the $NaHSeO_3$ to be fully bio reduced to selenium oxide nanoparticles via the oxidation of *S. cerevisiae*. To 90 ml of 2 mM $NaHSeO_3$, 10 ml of distilled water was added as the control sample. To generate a homogeneous mixture, both flasks were incubated for three hours in the dark on a rotary shaker. The color of the solution varied. The produced color solution allowed the absorbance to be tested against various wavelengths to confirm the production of Sc-SeNPs.

2-9 Characterization and examination of ScE/Selenium nanoparticles (Sc-SeNPs)

The ScE/Selenium nanoparticles were characterized in this study via some examinations as the following:

UV-Vis absorption spectroscopy

UV-Vis double-beam spectrophotometers were utilized to measurement the absorbance spectrum of the yeast extract nano selenium solution. Every spectrum was recorded at room temperature in a quartz cell with a 1 cm optical path. Deionized distilled water was used as a control. (200–800 nm) was used to compute the absorption [19]. The Ministry of Science and Technology-Iraq checked the measurements.

Fourier Transform Infrared (FTIR) Spectroscopy Analysis

Fourier Transform Infrared (FTIR) analysis was used to characterize the functional groups on the surface of the yeast extract containing nanoselenium. The spectra were scanned at a resolution of 4 cm-1 within the 400–4000 cm-1 range. The samples were created via normal procedures by spreading them on a microscope slide [20].

Atomic force microscopy (AFM)

Under standard air conditions, the surface morphology of the nanoparticles was observed via an atomic force mreicroscope in contact mode, under normal atmospheric conditions [21]. The measurements of this test were done in Iran at the University of Kashan.

Field emission - Scanning electron microscopy (feSEM) analysis

The shape of the produced nanoparticles was examined by scanning electron microscopy (SEM). The materials were examined under a Brucker scanning electron microscope to determine their morphology. Standard procedures of Atangana *et al.,* [22] were followed in the preparation of the samples at the University of Kashan.

X-ray diffraction (XRD)

Each type of nanoparticle was evenly suspended in a thin layer of water on a glass slide, which was then allowed to dry. X-ray diffraction (XRD) patterns were acquired with an X-ray diffractometer set to $2\theta/\theta$ scanning mode (operational voltage, 40 kV, current, 30 mA, and Cu K (a) radiation, $\lambda = 1.540$). The XRD pattern was observed in the 2θ range of 10 to 80 degrees with a step of 0.02 degrees in a fixed time mode at room temperature [23]. This analysis was conducted at the University of Kashan / Iran.

2-10 The antibacterial activity of ScE and Sc- SeNPs was assessed by MIC via the microtiter plate method (MTP).

The assay was designed to test the minimum inhibitory concentrations (MICs) of ScE were (250, 125, 62.5, 31.25, 15.625, 7.8125, 3.9062, 1.9531, 0.9765and 0.4882 μg/ml) and Sc-SeNPs

(440, 220, 110, 55, 27.5, 13.75, 6.875, 3.4375,1.7187, and 0.8593 µg/ml)against six isolates of *S. aureus* (S13, S14, S21, S33, S35, and S36) which were selected because of their formation of strong biofilms and have multidrug resistance , In accordance with Abduljabar and Hussein [24], a 96-well microtiter plate supplemented with resazurin dye in Mueller–Hinton broth (MHB) was used.

2-11 Inhibitory effectiveness of ScE and Sc-SeNPs against S. aureus biofilm formation.

The microtiter plate (MTP) assay is a qualitative method for biofilm assessment, and it was used to assess the ability of ScE and Sc-SeNPs to prevent the production of biofilms via a microplate reader using the MIC from the prior experiment, to inhibition the biofilm development of the studied *S.aureus* isolates. The quantification of biofilm formation was assessed according to guidelines provided by Haney *et al*., [25]. An ELISA microplate reader was used to measure the absorbance of each well at 600 nm, and the optical density of each well was determined. The biofilm formation of the isolates was ascertained via blank absorbance measurements. Isolates that develop biofilms are those whose OD values are higher than those of the blank well. Using the cut-off value (ODc), isolates can be categorized as producers of biofilms.

ODc: (3x standard deviation (SD) of the negative control plus the average OD of the negative control).

OD isolation: ODc is the average OD of the isolate.

On the basis of the OD values found for each unique bacterium, the following classification of bacterial adherence: was used: Optical density (OD) <= ODc (non-adherent), 2ODc> OD> ODc (weak), 4ODc> OD> 2ODc (moderate), and OD> 4 ODc (strong).

On the other hand, 100 µl of each test compound was added was given. The plate was incubated at 37°C for 24 h. After that, a microplate reader was used to clean, stain, and read each well at 600 nm. The degree of biofilm inhibition was determined via the following equations [26]:

[(OD Control-OD Sample) /OD Control] ×100 = % Biofilm inhibition

2.12- Statistical analysis

The statistical calculation of the results was performed via Microsoft Excel 2019, one-way ANOVA, a p- value for the probability of $P<0.05$, and the least significant difference (LSD) test for comparison.

4- Results and discussion

A total of 150 clinical samples were collected from three hospitals in Baghdad. Only, thirty-six isolates grown directly on mannitol salt agar and blood agar were identified by the presence of beta-hemolytic colonies on blood agar and yellow (golden) colonies that resulted from the fermentation of mannitol sugar, which turned phenol red golden. These results revealed typical morphological traits of *S. aureus.*

The isolates were subjected to standard biochemical tests. These isolates were positive for catalase and coagulase reactions. However, the oxidase tests yielded a negative result. According to the findings, only 36(24%) samples received standard biochemical testing and *Staphylococcus aureus* -specific morphological features. The distribution of sample proportions was as follows: wound 10 (27%), urine 16 (41%), burn 1 (2%), sputum 4 (11%), nasal swab 2 (5%), throat swab 1 (2%), and CSF 2 (5%). These results agree with those of Ahmed and Al-Daraghi [27], who reported that 15 *S. aureus* isolates were isolated from UTIs and 9 from wounds. These samples

also gave a 100% positive result for the *16S rRNA* gene as a genetic identification of *S. aureus* via PCR, which agreed with the results of Shamkhi *et al.,* [28] and 97.22% positive results for *mecA* as methicillin-resistant *S. aureus* isolates, which agreed with the results of Kadhum and Abood [29].

4-1 Molecular identification of Staphylococcus aureus

Detection of 16SrRNA

The results of the PCR reaction by gel agarose electrophoresis showed that 36 (100%) of *S. aureus* isolates were positive for the *16S rRNA* gene (578 bp), as shown in Figure (1). These results are in agreement with Ajani *et al*., [30].

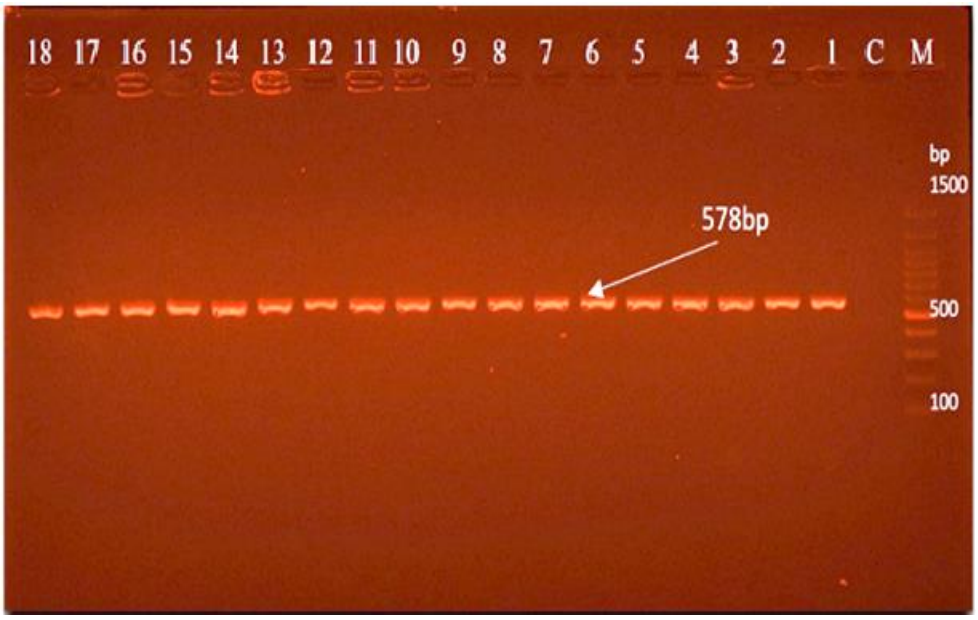

Figure 1: Agarose gel electrophoresis of amplified PCR product for the detection of *16SrRNA* gene (578bp) run on 1.5% agarose (80 min at 70 volt) stained with ethidium bromide, lane 1-18 *S. aureus* isolates; M: Marker DNA ladder (100bp) and C: Negative control.

Detection of mecA gene

The *mecA* gene was confirmed by agarose gel electrophoresis and photographed under an ultraviolet trans illuminator, shown in Figure 2, where the amplification revealed a product of 163bp. The rate of clinical *S. aureus* isolates that gave a positive result for the *mecA* gene was (97.22%). These results are in agreement with the research of Al-Dahbi and Al-Mathkhury [31].

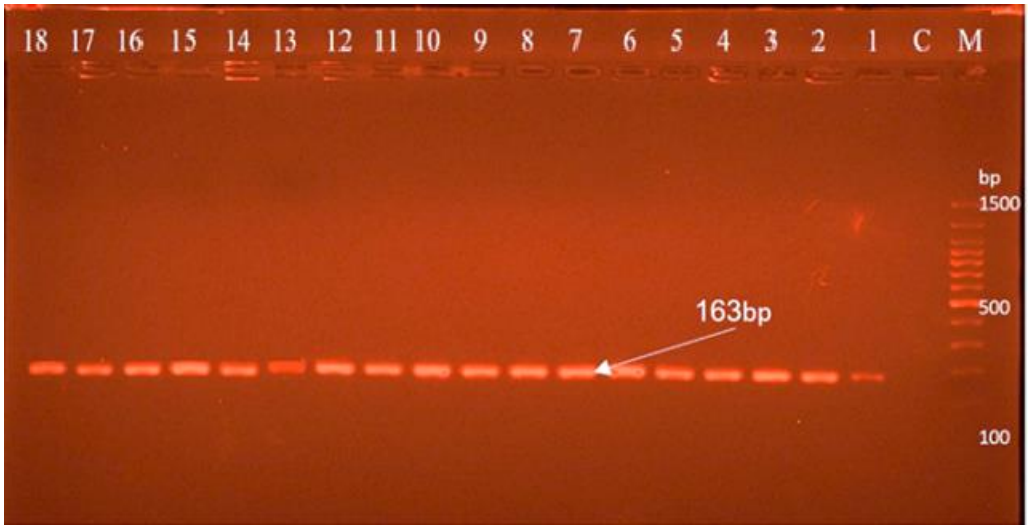

Figure2: Agarose gel electrophoresis of amplified PCR product for the detection of *mecA* gene (163bp) run on 1.5% agarose (75 min at 70 volt) stained with ethidium bromide, lane 1-18 *S. aureus* isolates; M: Marker DNA ladder (100bp) and C: Negative control.

4-2 Identification of S. cerevisiae

Morphological findings following three days of incubation at 30°C on potato dextrose agar (PDA) revealed that colonies that seemed to be yeasts exhibited distinct earthy odors. Additional features included a color range of cream to white cream, an oval to circular microscopic shape, irregularity, and the occurrence of yeast isolates alone [32]. Both single and paired budding characteristics were present in the yeast isolates (Figure 3).

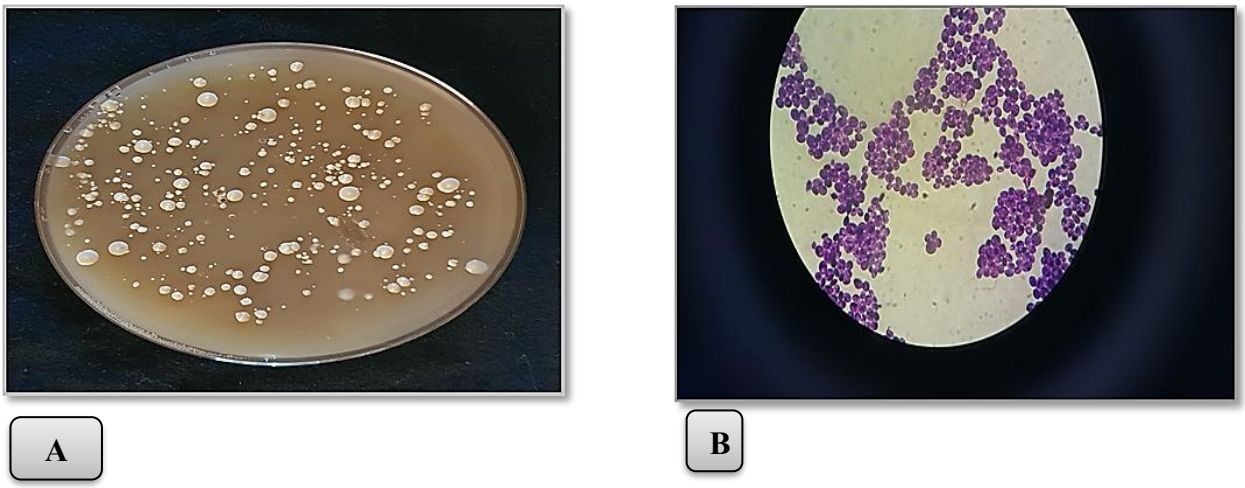

Figure 3 : A: Colonies of *S. cerevisiae* growing for 3 days at 30°C on PDA agar. B: Budding form of *S. cerevisiae* under a microscope

4-3 Molecular identification of S. cerevisiae.

ITS-PCR with an 880 bp PCR amplicon was used to separate yeasts belonging to the genus Saccharomyces from the other non-Saccharomyces species [33]. As shown in Figure (4), the PCR result revealed that the *S. cerevisiae* isolate tested positive for the *ITS* gene.

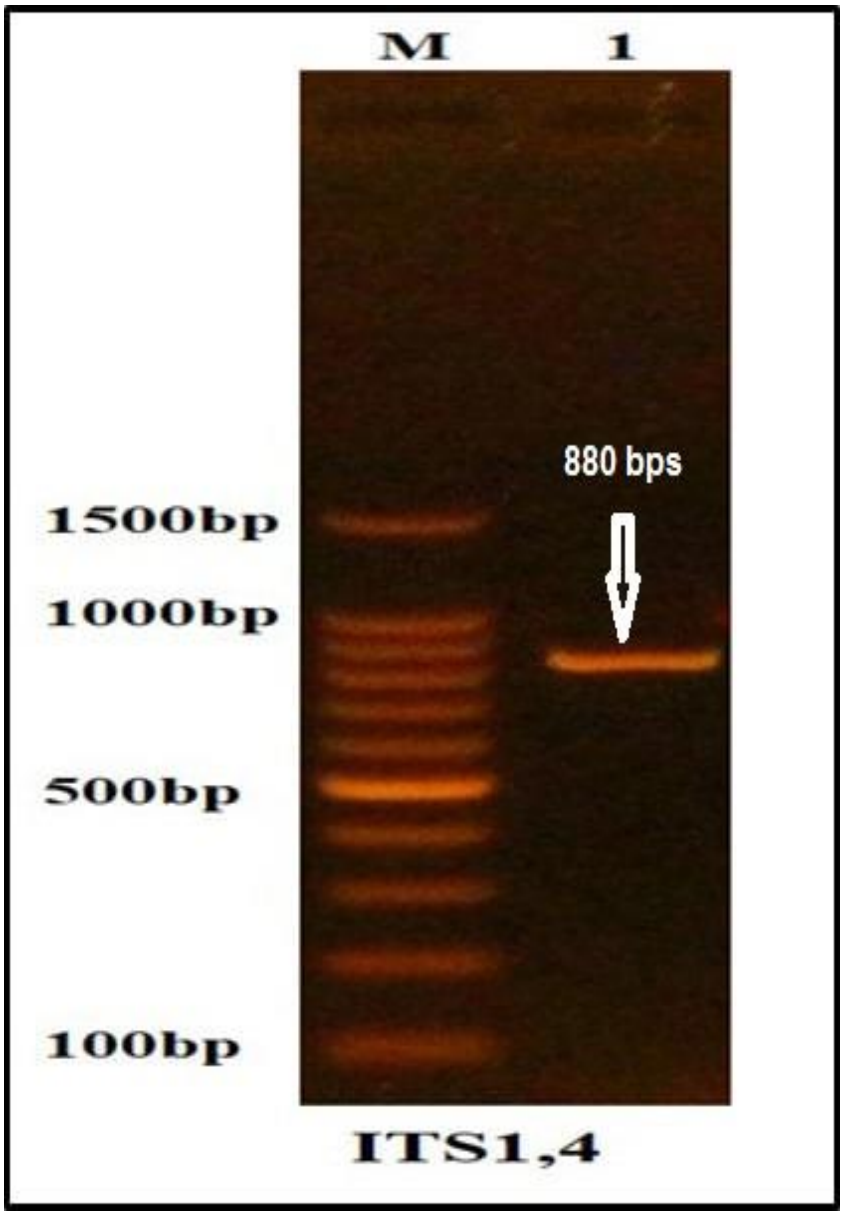

Figure 4 : *S. cerevisiae ITS* gene 880 bp amplification result was separated via 1.5% agarose gel electrophoresis and stained with ethidium bromide M: 100 bp ladder marker. Lane 1 shows the results of PCR.

4-4 preparation of Saccharomyces cerevisiae extract

After free-cell supernatant aqueous extract was placed in a glass petri dish in an oven at 40 ºC to dry, the remaining total weight of free-cell supernatant aqueous extract was 19.88g.

4-5 GC–MS analysis of the Saccharomyces cerevisiae extract.

The chemical compounds found in the *S. cerevisiae* free-cell supernatant aqueous extract, retention duration (R.T.), and percent composition area were identified via gas chromatography with mass spectrometry. The results revealed the presence of 19 chemicals, which are displayed in Figure (5) and Table (1).

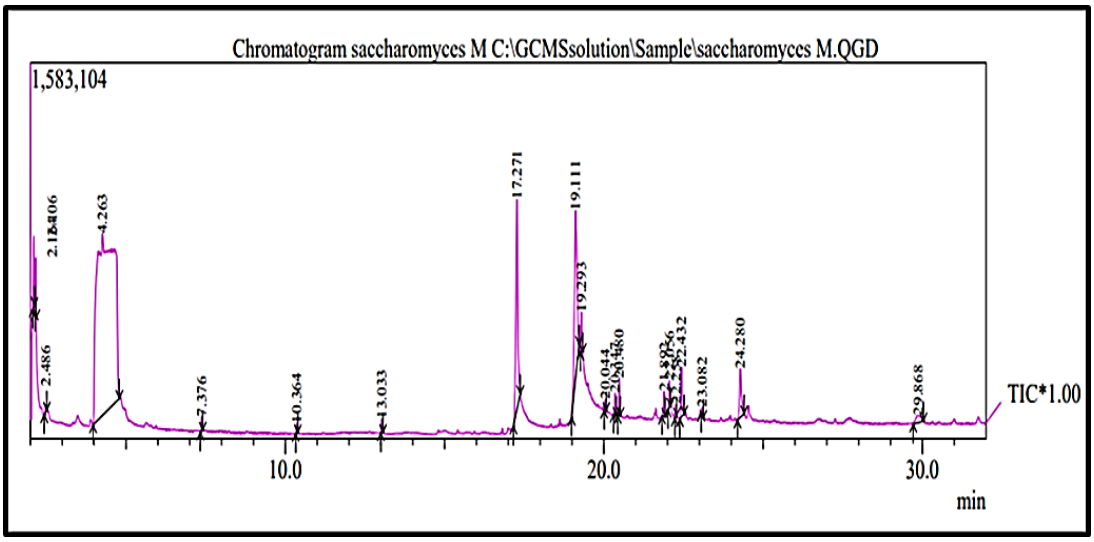

Figure 5 : GC- histogram analysis of *S. cerevisiae* extract.

Table 1: Chemical compounds of the ScE *S. cerevisiae* extract.

R.T.	Area%	Component name	Chemical compounds
2.164	0.80	Muramic acid	Flavonoid
2.486	0.21	3-Piperidinol	Alkaloid
4.236	70.26	o-Ethylhydroxylamine	Alkaloids
7.376	0.28	Oxalic acid, isobutyl pentyl ester	Terpenoids
10.364	0.18	Oxalic acid, isobutyl pentyl ester	Terpenoids
13.033	0.26	Coumarin, 8-acetyl-7-hydroxy-4-methyl	Coumarine
17.271	9.02	Palmitic acid	Flavonoid
19.111	9.66	delta.(Sup9)-cis-Oleic acid	Flavonoid
19.293	0.95	delta.(Sup9)-cis-Oleic acid	Flavonoid
20.044	0.22	Pentafluoropropionic acid,tridecyl ester	Terpenoids
20.347	0.43	2-(dimethylamino)ethyl ester	Terpenoids
20.480	0.71	Pentafluoropropionic acid, tridecyl ester	Terpenoids
21.892	0.60	2-(dimethylamino)ethyl ester	Terpenoids
22.056	0.46	Octadecenyl aldehyde	Steroid
22.258	0.22	Hexane, 1-(hexyloxy)-5-methyl	Resin
22.432	1.36	Pentafluoropropionic acid,tridecyl ester	Terpenoids
23.082	0.12	3-Methyl-1-hexanol	Resin
24.280	2.18	delta.(Sup9)-cis-Oleic acid	Flavonoid
29.868	0.83	Fumaric monoamide, N-(2-bromophenyl)-, nonyl ester	Terpenoid

o-Ethylhydroxylamine, the primary component of ScE and a member of the alkaloid group, presented the highest concentration in the *S. cerevisiae* extract, accounting for 70.26% of the overall peak area during the retention period (4.236) min. In addition, delta (Sup9)-cis-oleic acid had a peak area of 12.79% in three different retention periods (19.111, 19.293, and 24.280 minutes), and palmitic acid had a peak area (9.02%) in the retention time (17.271) minutes; these two chemicals are flavonoids. After that, the peak area progressively decreased. There were compounds that emerged frequently over varying lengths of time, and the compounds'

appearance times fluctuated. Compared with the findings of Makky *et al*., [34], we discovered that 1,2-benzenedicarboxylic acid mono(2-ethylhexyl) ester, a member of the terpenoid group, was the primary constituent of the *S. cerevisiae* ethyl acetate extract. This could be because the yeast extract used in this study is alcoholic, in contrast to our research, where the yeast extract is aqueous. Research by Barati and Chahardehi [35]. Revealed that alkaloids have a range of biological effects, including anti-inflammatory, anticancer, antifungal and antibacterial effects. In addition to the medicinal efficacy of ScE its primary constituent is an alkaloid that suppresses bacterial growth in multiple ways, including (i) binding to DNA and RNA to block bacterial nucleic acid and protein production [36]; (ii) alkaloids have the ability to function as efflux pump inhibitors (EPIs) against MRSA [37]; and (iii) the inhibition of bacterial metabolism involves interference with the energy and primary metabolism of bacteria to prevent their growth or block their production of toxins. One of the possible targets is adenosine triphosphate (ATP) [38]. Also, alkaloids stop bacterial functional proteases from acting, interfering with respiration and DNA topoisomerase [39]. Additionally, the polyphenols found in ScE have antibacterial effects on bacteria via a variety of mechanisms, including interactions with proteins and bacterial cell walls, modifications to cytoplasmic functions and membrane permeability, suppression of energy metabolism and DNA damage, and suppression of bacterial cell synthesis of nucleic acids [40]. In conclusion, adding long aliphatic chains to flavonoids increases their hydrophobicity, making it easier for the compounds to interface with the bacterial cytoplasmic membrane and increasing their antibacterial activity.

4-6 Visual confirmation

SeNP generation was first observed and confirmed visually. Figure (6B) shows how the color changed from clear to brownish after adding 10 ml of *S. cerevisiae* extract to 90 ml of 2 mM $NaHSeO_3$ separately at a flow rate of 0.2 ml/min. However, after incubation for three hours in the dark on a rotary shaker, the brownish solution turned orange and further changed into deep brick orange colour as shown in Figure (6c). The colour changes indicated the formation of colloidal SeNPs. These colour changes indicate the initial assumption of SeNPs formation as the selenium oxyanion (Se_3^{2-}) reduced to elemental selenium (Se^0).

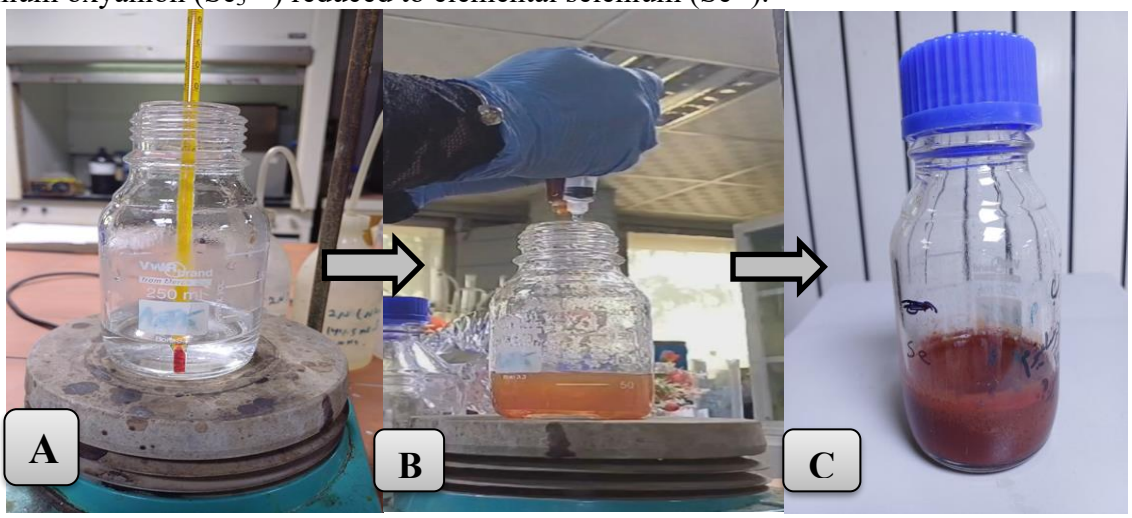

Figure 6 : Stages of the preparation of SeNPs via ScE. A: 90 ml of 2 mM NaHSeO3 solution B: 10 ml of yeast was added to 90 ml of 2 mM NaHSeO3 separately at a flow rate of 0.2 ml/ min C: Solution containing *S. cerevisiae* extract loaded on selenium nanoparticles.

4-7 Characterization of the Sc-SeNPs

UV-Visible spectroscopy

UV–visible spectroscopy is a primary step in the confirmation of the synthesis of Sc-SeNPs. The absorbances of ScE and Sc-SeNPs were measured.The results are shown in Figure (7) and Table (2) for ScE and for Sc-SeNPs, as shown in Figure (8) and Table (2).

Table 2: UV--visible spectral analysis results of the ScE and Sc-SeNPs

Peak no.	Wave length nm	ScE	Sc- SeNPs
1	287.00	4.000	0
2	284.00	0	2.169
3	276.00	3.957	0
4	266.50	3.607	0
5	256.00	0	0.166
6	252.00	0	2.157
7	242.00	2.278	0
8	216.50	0	0.431

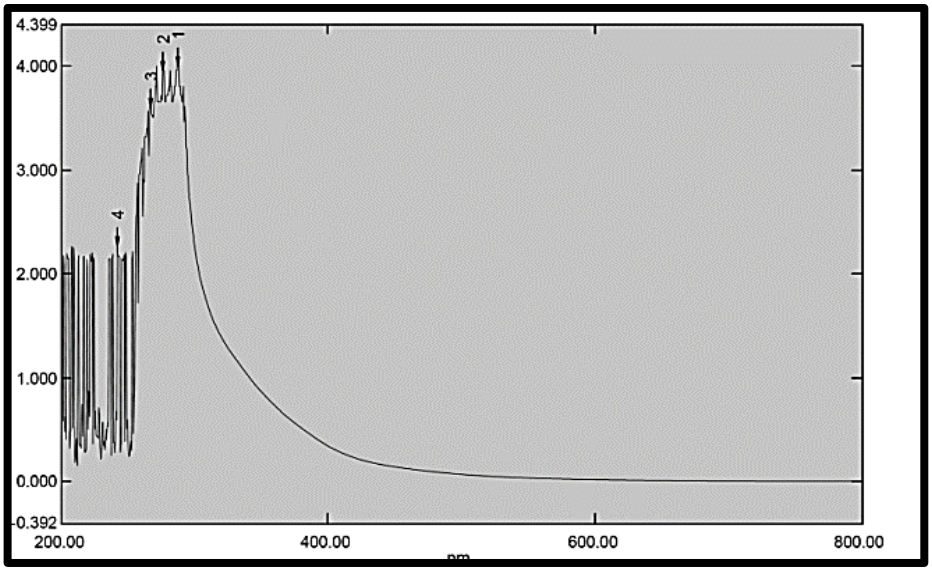

Figure 7 : UV-Visible spectral analysis of ScE

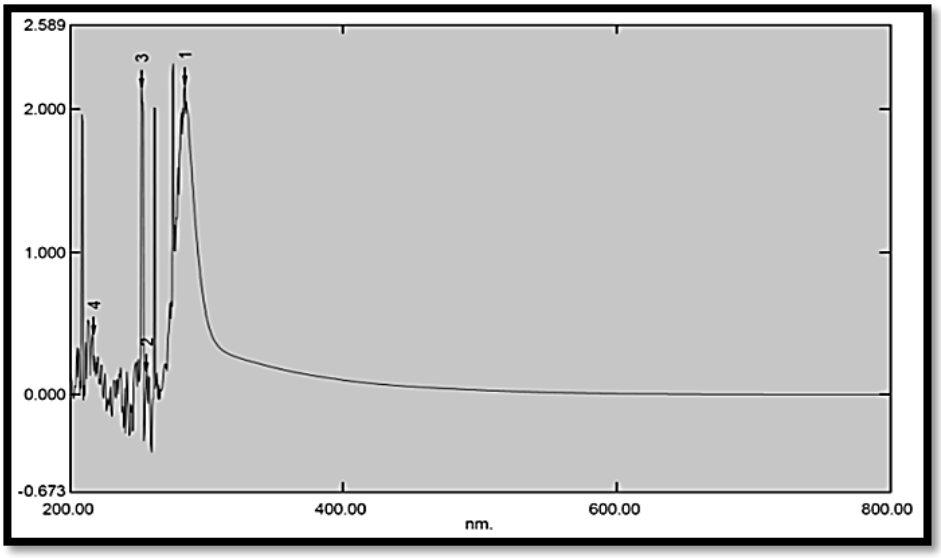

Figure 8: UV-Visible spectral analysis of Sc-SeNPs

Along with the disappearance of the wavelength (287.00) nm from the Sc-SeNPs and the new wavelength with high absorbance at (284.00) nm in the Sc-SeNPs material, the highest absorbance value in the Sc-SeNPs material at a wavelength of (284.00) nm, with a value of (2.169), followed by the highest value in the ScE at a wavelength of (287.00) nm, with a value of (4.000), indicates the formation of the nanomaterial and the successful loading of the extract on the selenium nanoparticles.

Fourier transform infrared spectroscopy (FTIR)

Through FTIR analysis, the substances in the *S. cerevisiae* extract that served as reducing, stabilizing, and capping agents were identified. In the 400–4000 cm-1 range, as shown in Figure (8), FTIR analysis was carried out. At 615.29 cm-1, 1398.39 cm-1, and 1653.00 cm-1, novel spectra corresponding to the groups (alkynes, aromatics, and alkenes) were observed when the spectra of the ScE and Sc-SeNPs were first compared. Owing to the interaction of *S. cerevisiae* with selenium nanoparticles, these peaks were not present in ScE, suggesting the formation of a new link. Furthermore, the center peak of the Sc-SeNPs, which is at 3402.43 cm-1 and belongs to alcohols and phenols, showed that phenolic compounds include hydroxyl groups, which are responsible for converting the selenium oxyanion to elemental selenium, which in turn forms selenium nanoparticles. These results are consistent with those of Radzi *et al*., [41].

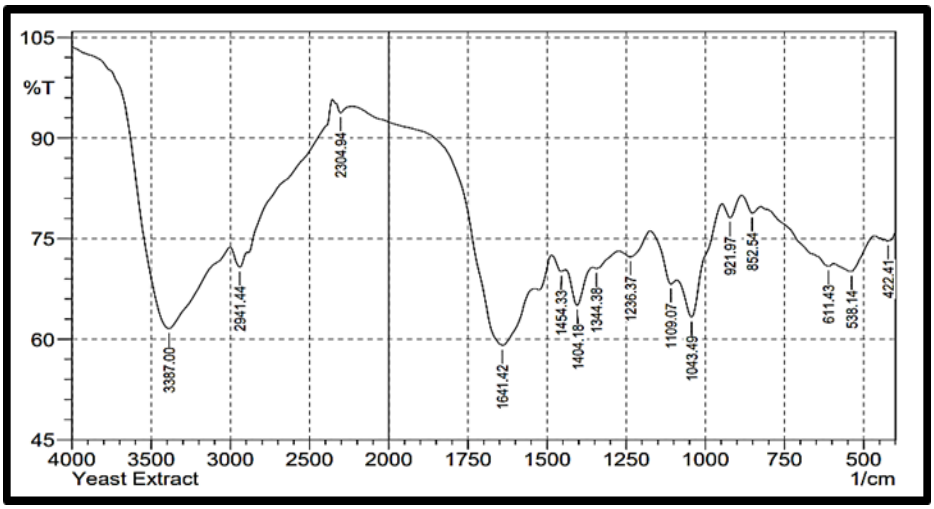

(A)

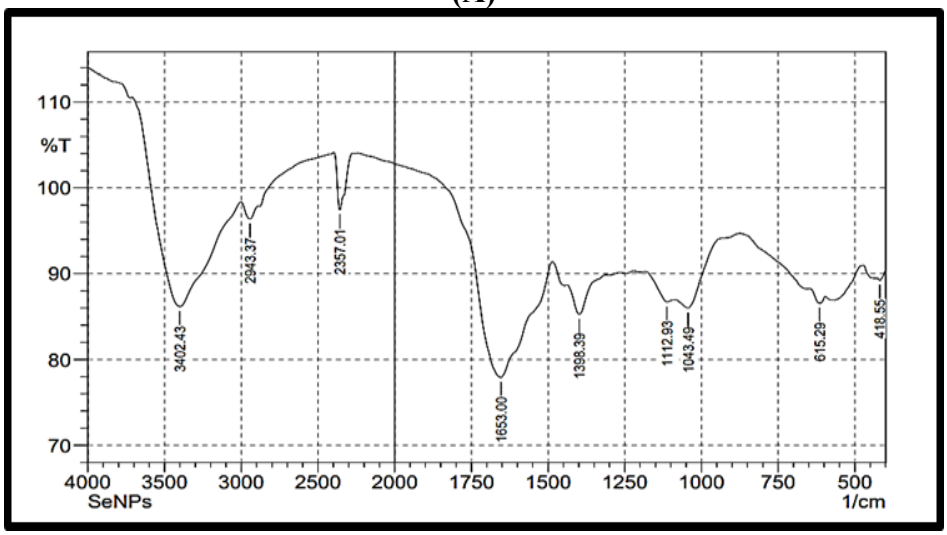

(B)

Figure 8 : (A) FTIR spectra of the yeast extract, (B) FTIR spectra of the Sc-SeNPs

- **Atomic force microscopy (AFM) analysis**

Atomic force microscopy images were employed to quantify the diameters of the particles and the surface topography of the Sc-SeNPs; the largest particles measured varied in size from 54.04 nm. The dispersion of the Sc-SeNPs according to the particle size is shown in Figure 9.

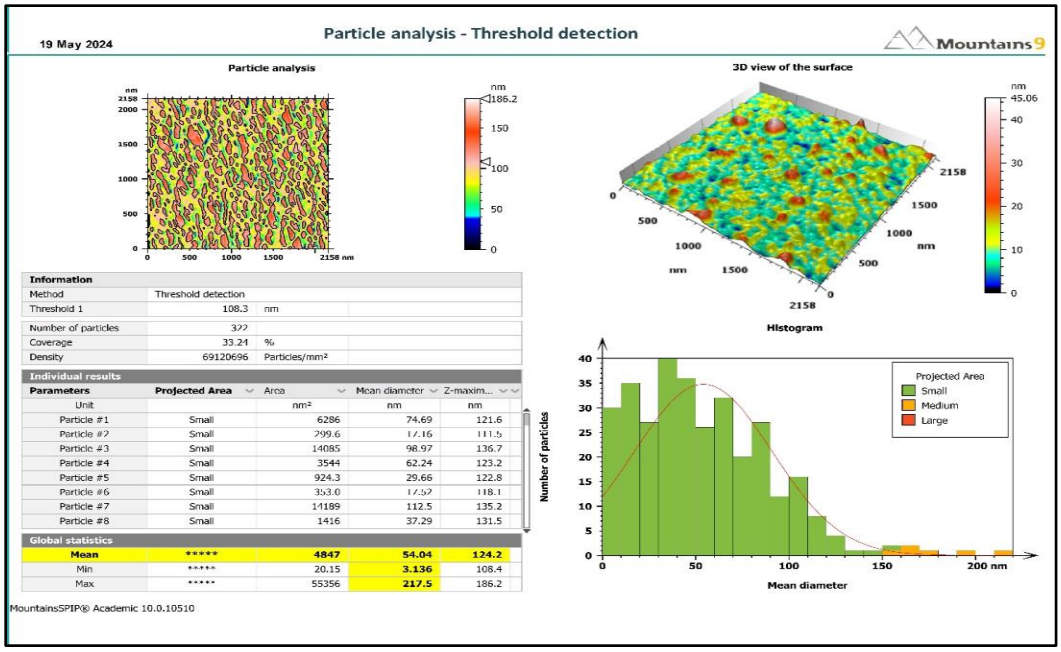

Figure 9 : The particle size of Sc-SeNPs.

Field emission - Scanning electron microscopy (SEM) analysis

The morphology of the Sc-SeNPs was examined via feSEM; the findings are shown in Figure (10). The Sc-SeNPs have a relatively uniform morphology and a spherical appearance with a diameter range of 30.89–50.01 nm. These findings corroborated those of Hasan *et al*., [42], who reported that homogeneous particles with an average size of 60±15 nm were present in morphologically mediated selenium.

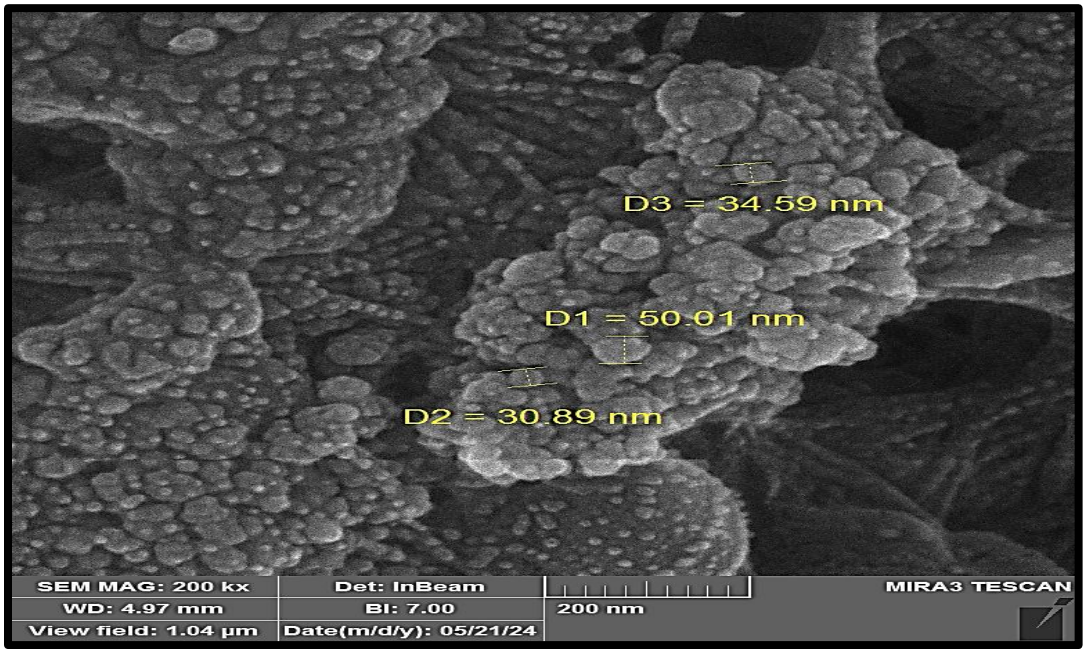

Figure 10 : SEM image of the Sc-SeNPs.

X-ray diffraction (XRD)

Figure (11A) displays the Sc-SeNPs peak, with its primary 2θ value peak located at 31.9705° and an intensity level of 736.5503 cont. This result agrees with Aftab *et al.,* [43], who displayed the X-ray diffraction patterns of selenium with the center peak of the 2θ value at 30.3° (Figure 11B). This shift shows that the crystal structures of the two materials differ, with Sc-SeNPs having a more crystalline structure than selenium.

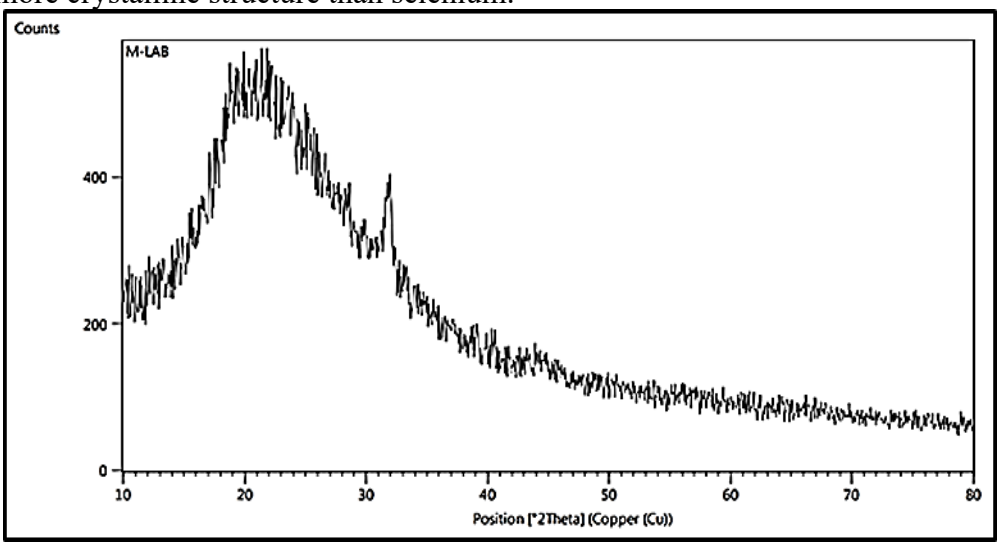

(A)

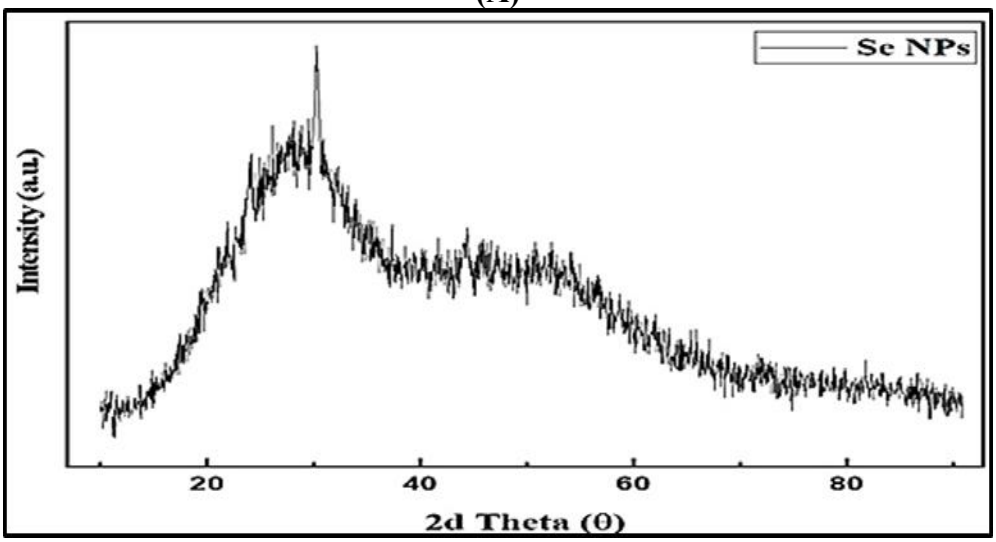

(B)

Figure 11 : A:Diffractogram of Sc-SeNPs , B:Diffractogram of SeNPs.

4-8Antibacterial activity of ScE and Sc-SeNPs via the MTP method

Minimum inhibitory concentrations (MICs) of *S. aureus* isolates in comparison with those of the control group. All of the test wells were blue at first, but after two to four hours of incubation, a few of them developed a pink color, which may indicate the growth of bacteria, as shown in Figure 12 and Table 3. The presence of alkaloids and polyphenols, which act as antibacterial agents through many pathways as previously described, is responsible for the greater antibacterial activity of the Sc-SeNPs (440, 220, and 110 µg/ml) than the ScE at (125 mg/ml).

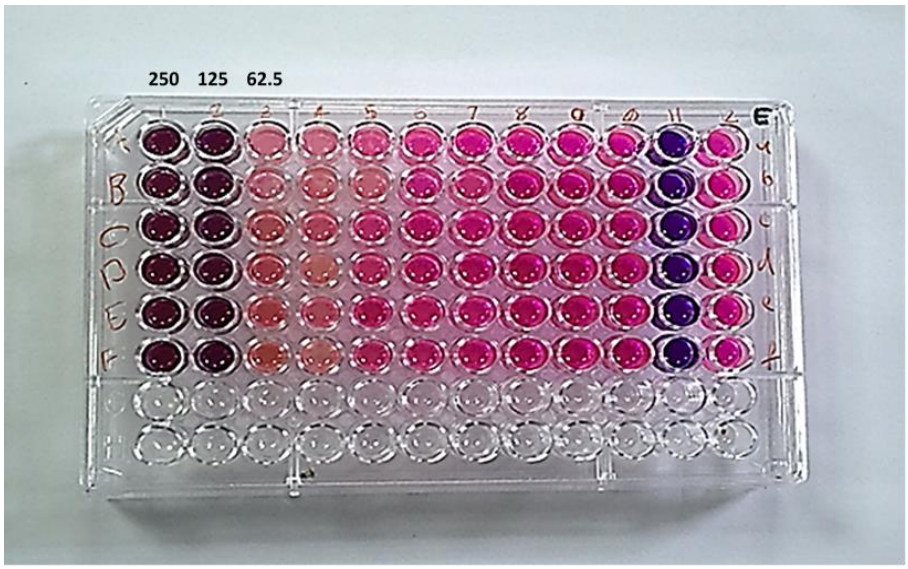

(A)

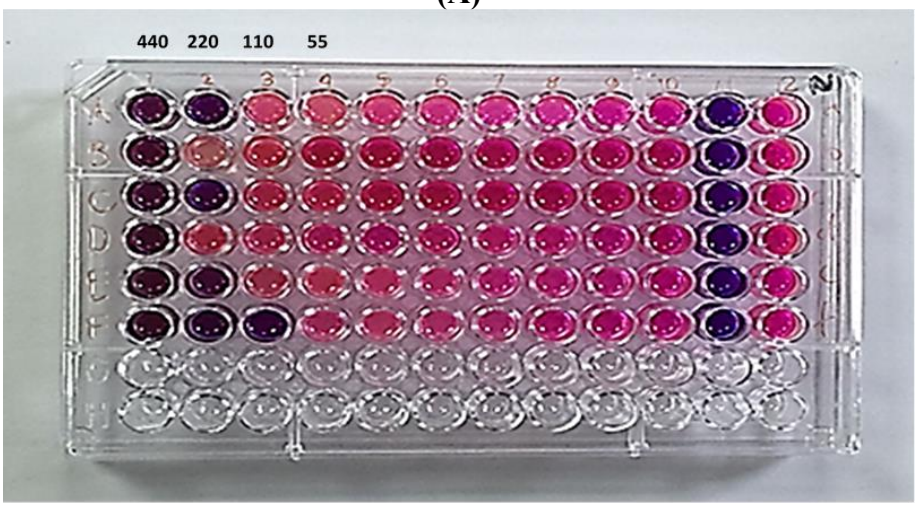

(B)

Figure 12 : (A)Microtiter plate with 96-wells of ScE alone on *S.aureus* . (B) Microtiter plate with 96-wells of Sc-SeNPs on *S.aureus*

Table 3 : MICs of Sc-SeNPs and SCE determined via the resazurin-aided microdilution method against *S. aureus*.

Isolates code	ScE MIC (mg/ml)	Sc-SeNPs MIC (µg/ml)
S13	125	440
S14	125	440
S21	125	220
S33	125	220
S35	125	220
S36	125	110
LSD value	0.00 NS	32.907 *

* (P≤0.05).

The Sc-SeNPs and SCE MIC values (P≤0.05) were compared and statistically assessed. The efficacy of ScE and Sc-SeNPs differed, suggesting that there were significant differences between the two groups. The MIC for the Sc-SeNPs varied from 440 to 110 µg/ml, whereas the MIC for ScE was 125 mg/ml. These were the ideal numbers for preventing the growth of *S. aureus*. This is because the nanoparticles are more abundant and smaller in size than normal extracts are, which allows us to prepare a nanoextraction at a lower concentration and, hence, at a lower cost. These findings are consistent with earlier research by Salem *et al*., [18], who reported that *S. aureus* was the most susceptible bacteria to Se-NPs at 1000 µg/ml and an MIC of 25 µg/ml.

4-9 Determination of the effectiveness of antimicrobial agents in preventing biofilm formation

A microplate reader was used to evaluate the effectiveness of the ScE and Sc-SeNPs against biofilm formation. Using minimal inhibitory concentrations of ScE and Sc-SeNPs, the effects of the test substances on the formation or inhibition of biofilms of the studied *S. aureus* isolates (S13 to S36) that create strong biofilms were examined. as shown in Table (4).

Table 4 : Optical density of Sc-SeNPs and ScE against the biofilm production of *S.aureus* isolates

Isolates	Control biofilm (%)	Inhibition SeNPs loaded ScE (%)	Inhibition ScE (%)	LSD value
S13	100	63.75	36.91	7.749 *
S14	100	87.37	35.82	9.512 *
S21	100	22.69	34.96	7.028 *
S33	100	55.44	73.26	7.984 *
S35	100	92.85	35	9.577 *
S36	100	95.74	79.1	8.137 *
LSD value	---	8.934 *	8.025 *	---

* (P≤0.05).

When the MICs of ScE and Sc-SeNPs were compared and statistically assessed (P≤0.05), the efficacies of ScE and Sc-SeNPs differed from one another. The Sc-SeNPs demonstrated high inhibitory activity, ranging from 22.69% to 95.74%, while the inhibition of ScE varied from 34.96% to 79.1%. These findings are consistent with the findings of Salem *et al*.,[18], who described that the percentage of SeNPs that inhibited *S. aureus* biofilms ranged from 62.5% to 88%.

Discussion

The crucial trace element selenium has demonstrated strong antibacterial in its nanoscale form [44]. Compared with other synthesis methods, biosynthesized selenium nanoparticles (SeNPs) exhibit less cytotoxicity toward normal cell lines, rendering them desirable materials for use in human investigations, arthritis, and nephropathy, because of their low toxicity and anticancer qualities [45]. Numerous bacterial and fungal infections, including *S. aureus*, have been reported to be effectively treated by SeNPs by Nguyen, *et al*., [46]. Living organisms are vulnerable to microbial infections, which can result in a variety of diseases that pose serious health risks. Currently, the majority of pathogenic organisms are resistant to drugs [47]. Because

SeNPs are antibacterial, they effectively fight against bacterial illnesses that are resistant to several drugs by dismantling bacterial structures, suggesting potential antibiotic substitutes [48].

The antibacterial activity of nanoparticles is correlated with their size, with smaller particles having greater stability and an excess surface-to-volume ratio that promotes intracellular diffusion and effective interactions [49]. The larger contact surface area and smaller size of SeNPs between 40 and 60 nm allow them to more easily pass through the bacterial membrane and cell wall, causing cell lysis, disrupting ATP synthesis, and influencing cell division, ultimately resulting in bacterial cell death [50]. This is the reason for the higher antibacterial activity observed in this work. Se NPs enhance the antibacterial activity of lysozymes, which have the ability to combat infections, according to a study that examined the synergy between Se NPs and lysozymes [51]. Anti-infection drugs are thus created to treat these incurable illnesses. Many metal oxides, metal nanoparticles, and their combinations have been identified as possible antibacterial agents. Additionally, SeNPs have shown great promise in the biomedical field as antibacterial agents to guard against microorganisms on implanted clinical devices. Inserted SeNPs into common polymers, such as silicon, polyvinyl chloride, and polyurethane, which are typically utilized in biomedical devices, via an in-situ technique. They reported that the concentration of selenium in the coating material, when combined with various polymers, was directly correlated with the antibacterial performance. According to some researchers, uncoated polymers can effectively promote *S. aureus* growth whereas nanoselenium-coated polymers cannot. Furthermore, they reported that SeNP-covered polyvinyl chloride (PVC) exhibited stronger antibacterial properties than Ag-covered PVC, which is sold commercially [52]. According to Shakibaie, *et al*., [53] selenium nanoparticles inhibited the biofilm of *S.aureus* by 42%, compared to that of non-treated samples. Also, the effect of temperature and pH on the biofilm formation in the presence of SeNPs and SeO_2 is evaluated. On the other hand, because the *S. cerevisiae* extract contains alkaloids and polyphenols, which act as antibacterial and antibiofilm agents via many mechanisms, the strain of *S. cerevisiae* loaded with selenium nanoparticles plays an antibiofilm role.

Conclusion

Chemical crosslinking of two biomolecules to form a stable structure is a biological method of producing antibacterial and antibiofilm nanoparticles that facilitate targeted delivery of antibacterial agents for clinical MRSA. *S. cerevisiae* -SeNPs may be considered alternative agents that are more effective than aqueous extracts alone and have the ability to decrease bacterial resistance and biofilm formation.

Conflicts of Competing Interest

The authors declare that they have no potential conflicts of interest.

Ethical approval

Ethical approval of isolates collection was obtained from the Baghdad hospitals administration affiliated with the Ministry of Health / Republic of Iraq, which numbered (2021/01), as well as after consent of patients.

Acknowledgement

My sincere thanks to the ministry of science and technology and great appreciation to department of Biology\ college of science for women\ University of Baghdad.

References

[1] H.S.A. Al- Hayanni, "Antimicrobil resistance in Staphylococci and detection of *mecA* and *blaZ* genes in *Staphylococcus aureus*, *Staphylococcus sciuri* and *Staphylococcus epidermidis* isolated from fresh beef," *Biochemical and Cellular Archives*, vol.21, no.1, pp. 1571-1577, 2021.

[2] Z. Khatoon, C.D. McTiernan, E.J. Suuronen, T.F. Mah, and E.I.J. Alarcon, "Bacterial biofilm formation on implantable devices and approaches to its treatment and prevention," *Heliyon*, vol. 4, no.12, 2018.

[3] S.T. Ahmed, N.M. Abdallah ,S.M.H. Al- Shimmary and A.M.S. Al-Mohaidi, "The role of genetic variation for *icaA* gene *Staphylococcus aureus* in producing biofilm ," *International Journal of Drug Delivery Technology* ,vol.11, no. 2, pp. 390-395, 2021.

[4] A.F. Haag, J.R. Fitzgerald, J.R. Penadés, "*Staphylococcus aureus* in Animals," *Microbiology spectrum*, vol.7, no.3, 2019.

[5] D. Missiakas and V.J.F. Winstel, "Selective host cell death by *Staphylococcus aureus*: A strategy for bacterial persistence," *Frontiers in immunology*, vol. 11, p. 621733, 2021.

[6] M. Parapouli, A. Vasileiadis, A.S. Afendra, and E. J. A. Hatziloukas, "*Saccharomyces cerevisiae* and its industrial applications," *AIMS Microbiology*, vol. 6, no. 1, p. 1, 2020.

[7] Y. Munjal, RK. Tonk and R. Sharma, "Analytical techniques used in metabolomics: A review," *Systematic Reviews in Pharmacy*, vol.13, no. 5, p.515-21,2022.

[8] S.M. Al-Shimmary, Z.H. Shehab, and E.H. Jassim ,"Synthesis and characterization of cerium oxide-bacteriocin nanohybride with synergistic biological activities," *Egyptian Journal of Basic and Applied Sciences*, vol.12, no.1,p.1–16, 2024.

[9] C. Ferro, H.F. Florindo and H.A. Santos,"Selenium nanoparticles for biomedical applications: from development and characterization to therapeutics," *Advanced healthcare materials*, vol.10, no.16, p.2100598,2021.

[10] C.Gallo-Rodriguez and J.B.Rodriguez, "Organoselenium compounds in medicinal chemistry," *Chemistry and chemical and life science engineering*, vol.19,no.17, p.e202400063,2024.

[11] P.M. Tille,"Baily & Scotts diagnostic microbiology," 14th (ed.), Elsevier:pp.1084, 2017

[12] M.K. Kumar, C.Tyagi, A. Sahu, N. Desai, J. Manjhi, K.C. Mohan, Y.P. Reddy, S.K.Tiwari, L.K. Tomar and V.K. Sharma, "Identification and Characterization of *Staphylococcus aureus 16S rRNA* gene isolated from different Food Specimens from South Indian Region," *Journal of drug delivery and therapeutics*, vol. 10, no. 5, pp. 24-32, 2020.

[13] M. Mehrotra, G. Wang, and W. M. Johnson, "Multiplex PCR for detection of genes for *Staphylococcus aureus* enterotoxins, exfoliative toxins, toxic shock syndrome toxin 1, and methicillin resistance," *Journal of Clinical Microbiology*, vol. 38, no.3, pp.1032-1035, 2000.

[14] J.A. Barnett, R.W. Payne and D.Yarrow, "Yeasts: Characteristics and Identification," 3rd Edition. Cambridge University Press, 1139 pages, 2000.

[15] S.H. Mohaisen, M.H. Ali, Z.H. Shehab, A. Al-Mayyahi, and A.J.A. Abdulhassan, "Effect of Ultraviolet light on the expression of *icaD* gene in *Staphylococcus aureus* local isolates in Iraq," *Archives of Razi Institute* ,vol. 76, no. 5, pp. 1221-1227, 2021.

[16] A. Ruiz-Marín, Y. Canedo-López, A. Narváez-García, and J.C.J. Robles-Heredia, "Production of ethanol by *Saccharomyces cerevisiae* and *Zymomonas mobilis* Coimmobilized: *proposal for the use of organic waste*," vol. 50, no. 5, pp. 551-563, 2016.

[17] O. Zarei, S. Dastmalchi, and M.J.I. Hamzeh-Mivehroud, "A simple and rapid protocol for producing yeast extract from *Saccharomyces cerevisiae* suitable for preparing bacterial culture media," *Iranian journal of pharmaceutical research*, vol. 15, no. 4, p. 907, 2016.

[18] S.S. Salem, M. S. E. Badawy, A. A. Al-Askar, A. A. Arishi, F. M. Elkady, and A. H. Hashem, "Green biosynthesis of selenium nanoparticles using orange peel waste: Characterization, antibacterial and antibiofilm activities against multidrug-resistant bacteria," *Life*, vol. 12, no. 6, p. 893, 2022.

[19] O.A. Radhi, I. Albandar, K. Alqaseer, and W. D. Shnain. "Selenium nanoparticles inhibit *Staphylococcus aureus*-induced nosocomial infection, cell death and biofilm formation," *Journal of Population Therapeutics and Clinical Pharmacology*, vol.30, no. 4, p.367-378,2023.

[20] S.M.H. Al-Shimmary and A.N.J. Al-Thwani, "Synthesis and Characterization of Selenium-Enterolycin-A Nanohybrid System and Its Promising Biological Activities," *BioNanoScience*, vol. 14, no. 5 pp.5203-5216, 2024.

[21] W.L. Du, Z.R. Xu, X. Y. Han, Y. L. Xu, and Z.G.J. Miao, "Preparation, characterization and adsorption properties of chitosan nanoparticles for eosin Y as a model anionic dye," *Journal of hazardous materials*, vol. 153, no. 12, pp. 152-156, 2008.

[22] E. Atangana, T.T. Chiweshe and H. J. Roberts, "Modification of novel chitosan-starch cross-linked derivatives polymers: synthesis and characterization," *Journal of Polymers and the Environment*, vol. 27, pp. 979-995, 2019.

[23] M. Anand, P. Sathyapriya, M. Maruthupandy, and A. H. Beevi, "Synthesis of chitosan nanoparticles by TPP and their potential mosquito larvicidal application," *Frontiers in Laboratory Medicine*, vol. 2, no. 2, pp. 72-78, 2018.

[24] A.M. Abduljabar and N.N. Hussein, "Biological Activities of Silver Nanoparticles and Synergism Effects with Lincomycin Conjugation," *Iraqi Journal of Science*, pp.6226-6241,2023.

[25] E.F. Haney, M. J. Trimble, and R. E. Hancock, "Microtiter plate assays to assess antibiofilm activity against bacteria," *Nature protocols*, vol. 16, no. 5, pp. 2615-2632, 2021.

[26] H.A. Shaghati, E.H. Jassim, and L. A. K. Al-Zubaidi, "Evaluation of the Inhibitory Activity of *Syzygium aromaticum* Extract -Chitosan Nanoparticles Against Biofilm Formation of *Klebsiella pneumonia*," *Bionatura*, vol. 8, no. 1, pp. 1-14, 2023.

[27] Z.F. Ahmed and W.A. Al-Daraghi, "Molecular detection of *medA* virulence gene in *Staphylococcus aureus* isolated from Iraqi patients," *Iraqi Journal of Biotechnology*, vol. 21, no. 1, 2022.

[28] G. J. Shamkhi, S. M. Saadedin, and K. A. Jassim, "Detection the prevalence of some chromosomal efflux pump genes in Methicillin resistant *Staphylococcus aureus* isolated from Iraqi patients," *Iraqi Journal of Biotechnology*, vol. 18, no. 3, 2019.

[29] H.H. Kadhum and Z.H. Abood, "*Staphylococcus aureus* incidence in some patients with a topic dermatitis in Baghdad city," *Iraqi Journal of Biotechnology* , vol. 21, no. 2, pp. 13-20, 2022.

[30] TA. Ajani, C.J. Elikwu, V.Nwadike, T. Babatunde, C.G. Anaedobe, O. Shonekan, CC.Okangba, A. Omeonu, B. Faluyi, T.E. Thompson, E. Ebeigbe, B.G. Eze, M.A. Ajani, K. Perelade, M. Amoran, P. Okisor, T. Worancha, J. Ayoade, E. Agbeniga, C. Emmanuel and C A. Coker, "Nasal carriage of methicillin resistant *Staphylococcus aureus* among medical students of a private institution in Ilishan-Remo, Ogun State, Nigeria," *African Journal of Clinical and Experimental Microbiology*, vol. 21, no. 4, pp.311-7,2020.

[31] A. Al-Dahbi and H.J. Al-Mathkhury, "Distribution of methicillin resistant *Staphylococcus aureus* in Iraqi patients and healthcare workers", *Iraqi Journal of Science*, vol. 54, no. 2, pp. 293-300, 2013.

[32] Y. S. Yuma, "Isolation and characterization of yeast as potential probiotics from fermented cereals dough", *Journal of Veterinary Medicine and Research* ,vol. 7, no. 6, pp. 1-7, 2020.

[33] H. Šuranská, D. Vránová, and J.J. Omelková, "Isolation, identification and characterization of regional indigenous *Saccharomyces cerevisiae* strains," *Brazilian journal of microbiology*, vol. 47, no. 1, pp. 181-190, 2016.

[34] E.A. Makky, M. AlMatar, M.H. Mahmood, O. W. Ting and W.Z. Qi, "Antioksidacijska antimikrobna aktivnost etil-acetatnog ekstrakta kvasca *Saccharomyces cerevisiae*," *Food Technology and Biotechnology*, vol. 59, no. 2, pp. 127-136, 2021.

[35] M. Barati and A.M. Chahardehi, "Alkaloids:The Potential of Their Antimicrobial Activities of Medicinal Plants," *Medicinal Plants-Chemical, Biochemical, and Pharmacological Approaches*: Intech Open, 2023.

[36] L. Othman, A. Sleiman, and R. M. J. F. i. m. Abdel-Massih, "Antimicrobial activity of polyphenols and alkaloids in middle eastern plants," *Frontiers in microbiology*, vol. 10, p. 911, 2019.

[37] M. Mohtar, S.A. Johari, A.R. Li , M.M. Isa , S. Mustafa , A.M. Ali and D.F. Basri, "Inhibitory and resistance-modifying potential of plant-based alkaloids against methicillin-resistant *Staphylococcus aureus* (MRSA),"*Current Microbiology*, vol. 59, pp. 181-186, 2009.

[38] M. Sobti, R. Ishmukhametov, A.G.J. Stewart, "ATP synthase: expression, purification, and function," *Protein Nanotechnology: Protocols, Instrumentation, and Applications*, pp. 73-84, 2020.

[39] Y. Pommier, E. Leo, H. Zhang and C. Marchand, "DNA topoisomerases and their poisoning by anticancer and antibacterial drugs," *Chemistry & biology* ,vol. 17, no. 5, pp. 421-433, 2010.

[40] M. Makarewicz, I. Drożdż, T. Tarko, and A.J.A. Duda-Chodak, "The interactions between polyphenols and microorganisms, especially gut microbiota," *Antioxidants*, vol. 10, no. 2, p. 188, 2021.

[41] A.M.M. Radzi, Z. I. A. Tarmizi, N. A. Ghafar, S.H.M. Talib, and E.D.M. Isa, "Green synthesis of selenium nanoparticles and its electrochemical properties," in E3S Web of Conferences: EDP Sciences , vol. 516, p. 02006,2024.

[42] M. Hasan, M.J. Kadhim, and M. J. Al-Awady, " The Impact of Berberine Loaded Selenium Nanoparticles on *K. pneumoniae* and *Candida albicans* Antibiotics Resistance Isolates", *Archives of Razi Institute*, vol. 78, no. 3, pp. 1005-1015, 2023.

[43] R. Aftab, S.Ahsan , A.Liaqat , M. Safdar ,M.F. Jahangir , M. Nadeem, M.A. Farooqi , T. Mehmood and A.Khaliq , "Green-synthesized selenium nanoparticles using garlic extract and their application for rapid detection of salicylic acid in milk", *Food Science and Technology*, vol. 43, p. e67022, 2023.

[44] A. Khurana, S. Tekula, M.A. Saifi, P. Venkatesh, C.J.B. Godugu," Therapeutic applications of selenium nanoparticles," *Biomedicine & Pharmacotherapy*, vol. 111, pp. 802-812, 2019.

[45] H. Alam, N. Khatoon, M. Raza, P. C. Ghosh, and M. J. B. Sardar, "Synthesis and characterization of nano selenium using plant biomolecules and their potential applications," *BioNanoScience*, vol. 9, pp. 96-104, 2019.

[46] T. H. Nguyen, B. Vardhanabhuti, M. Lin, and A. J. F. C. Mustapha, "Antibacterial properties of selenium nanoparticles and their toxicity to Caco-2 cells," *Food Control*, vol. 77, pp. 17-24, 2017.

[47] H. Grundmann, M. Aires-de-Sousa, J. Boyce, and E.J. Tiemersma, "Emergence and resurgence of meticillin-resistant *Staphylococcus aureus* as a public-health threat," *The lancet*, vol. 368, no. 9538, pp. 874-885, 2006.

[48] H.W. Han, K.D. Patal, G.H. Kwak, S.K. Jun, T.S. Jang, S.H. Lee, S.K. Jun, J.C. Knowles, H.W. Kim, H.H. Lee and J.H. Lee. "Selenium nanoparticles as candidates for antibacterial substitutes and supplements against multidrug-resistant bacteria", *Biomolecules*, vol. 11, no. 7, p. 1028, 2021.

[49] M.T.A. Alnuaimi, H.S.A. AL-Hayanni and Z.Z. Aljanabi ,"Green synthesis of gold nanoparticles from *Sophora flavescens* extract and their antibacterial effect against some pathogenic bacteria," *Malysian Journal of Microbiology*, vol.19,no.1, p.74-82, 2023.

[50] L. Gunti, R. S. Dass, and N.K. Kalagatur, "Phytofabrication of selenium nanoparticles from Emblica officinalis fruit extract and exploring its biopotential applications: antioxidant, antimicrobial, and biocompatibility," *Frontiers in microbiology*, vol. 10, p. 931, 2019.

[51] N. E. Eleraky, A. Allam, S.B. Hassan, and M. M.J. Omar, "Nanomedicine fight against antibacterial resistance: an overview of the recent pharmaceutical innovations," *Pharmaceutics*, vol. 12, no. 2, p. 142, 2020.

[52] P.A. Tran and T.J. Webster, "Antimicrobial selenium nanoparticle coatings on polymeric medical devices," *Nanotechnology*, vol. 24, no. 15, p. 155101, 2013.

[53] M. Shakibaie, H. Forootanfar, Y. Golkari, T. Mohammadi-Khors and, M.R.M. Shakibaie, "Anti-biofilm activity of biogenic selenium nanoparticles and selenium dioxide against clinical isolates of *Staphylococcus aureus*, *Pseudomonas aeruginosa*, and *Proteus mirabilis*," *Journal of Trace Elements in Medicine and Biology*, vol. 29, pp. 235-241, 2015.